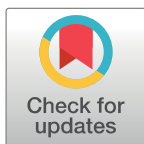# PLOS ONE

RESEARCH ARTICLE

Proteomic analysis of dorsal root ganglia in a mouse model of paclitaxel-induced neuropathic pain

Rania Hanna[1]◉, Alexandru Graur[2]◉, Patricia Sinclair ◉[1]◉, Bryan D. Mckiver[3], Paula D. Bos[4], M. Imad Damaj[3], Nadine Kabbani ◉[1,2]*

1 Interdisciplinary Program in Neuroscience, George Mason University, Fairfax, VA, United States of America, 2 School of Systems Biology, George Mason University, Fairfax, VA, United States of America, 3 Department of Pharmacology & Toxicology, Virginia Commonwealth University, Richmond, VA, United States of America, 4 Department of Pathology, Massey Comprehensive Cancer Center, Virginia Commonwealth University School of Medicine, Richmond, VA, United States of America

◉ These authors contributed equally to this work.
* nkabbani@gmu.edu

Abstract

Paclitaxel is a chemotherapy drug widely used for the treatment of various cancers based on its ability to potently stabilize cellular microtubules and block division in cancer cells. Paclitaxel-based treatment, however, accumulates in peripheral system sensory neurons and leads to a high incidence rate (over 50%) of chemotherapy induced peripheral neuropathy in patients. Using an established preclinical model of paclitaxel-induced peripheral neuropathy (PIPN), we examined proteomic changes in dorsal root ganglia (DRG) of adult male mice that were treated with paclitaxel (8 mg/kg, at 4 injections every other day) relative to vehicle-treated mice. High throughput proteomics based on liquid chromatography electrospray ionization mass spectrometry identified 165 significantly altered proteins in lumbar DRG. Gene ontology enrichment and bioinformatic analysis revealed an effect of paclitaxel on pathways for mitochondrial regulation, axonal function, and inflammatory purinergic signaling as well as microtubule activity. These findings provide insight into molecular mechanisms that can contribute to PIPN in patients.

Introduction

Paclitaxel is a taxane class compound used as a cytotoxic chemotherapy agent in the treatment of various solid tumors including prostate, ovarian, breast cancer, bladder, esophageal, small and non-small-cell lung, pancreas, and melanoma [1, 2]. Chemotherapy, with compounds such as paclitaxel, may interfere with a patient's course of treatment due to the emergence of pain symptoms in over 50% of cases [3]. There is no effective mechanism for the prevention of chemotherapy associated neuropathy and conventional analgesics and other pain medications are generally ineffective in negative symptom management [4].

Paclitaxel acts by disrupting proliferation of cancer cells through binding with β-tubulin [5] and suppressing its depolymerization. However, paclitaxel can also target non-cancer cells

leading to a number of side effects including skin toxicity like rash and pruritus [6], and neuronal toxicity associated with peripheral neuropathy [7]. Studies show that paclitaxel treatment causes changes in mitochondrial function, increased inflammation within dorsal root ganglia (DRG) and an increase in proapoptotic factors [7, 8].

The DRG is a primary sensory module consisting of sensory neurons, satellite glia, and immune cells such as macrophages and T cells [9]. Large DRG gives rise to myelinated axons that are involved in mechanoreception, whereas smaller DRG give rise to unmyelinated axons, which are involved in mechanoreception, thermoreception, and nociception [10]. Paclitaxel has been shown to traverse the blood-nerve barrier surrounding the DRG and bind microtubules within neurons, causing damage to axons and nerve fibers [11]. Microtubule stabilization underlies axonal transport loss, which promotes axonal degeneration, leading to peripheral neuropathy [12]. Paclitaxel induced peripheral neuropathy (PIPN) is associated with damage to sensory axons and nerve fibers in humans and animal models [13, 14].

Animal models exist to study molecular changes within sensory systems responding to paclitaxel exposure. Transcriptomic analysis of the DRG suggests an important role for paclitaxel in the activation of neuroinflammatory signaling within mice [14–16] however less is known about proteomic changes. In this study, we examined proteomic changes that may contribute to PIPN in a pre-clinical mouse model with heightened pain-like behaviors [17]. Specifically, the current proteomic analysis is conducted in mice that exhibit paclitaxel-induced mechanical hypersensitivity and cold hypersensitivity, as well as a decreased sensory nerve compound action potential (SNCAP) [17]. Our proteomic analysis aims to provide knowledge on mechanistic drivers of neuropathy during paclitaxel treatment.

Methods

Animals

The experiments were performed on 12-week-old male C57BL/6J mice (Strain #000664, The Jackson Laboratory, Bar Harbor, ME). Animals were housed in groups of 4 per cage with enriched environment and maintained on a 12 hour light/dark cycle, at a 22°C room temperature with ad libitum access to food (global 18% protein chow diet; Envigo Teklad, Indianapolis, IN, USA) and water. DRG from 8 animals for both the experimental and control groups were used, with 3 mass spectrometry technical replicates completed.

Ethical statement

All animal experiments were performed under an approved IACUC protocol in the Division of Animal Research of Virginia Commonwealth University (Richmond, VA), accredited by the Association for Assessment and Accreditation of Laboratory Animal Care (AALAC). All efforts were made to reduce the number of animals used in this study and to ensure optimal conditions of well-being before, during and after each experiment. Mice were observed daily for general well-being and their weight was measured weekly. All behavioral experiments were performed during the light cycle and with the observer unaware of the experimental treatment of the animals.

Drug treatment

Paclitaxel was purchased from VCU Health Pharmacy (Athenex, NDC 70860-200-50, Richmond, VA, USA) and dissolved in a 1:1:18 mixture of 200 proof ethanol, kolliphor, and distilled water (Sigma-Aldrich). Paclitaxel was administered at a dose of 8 mg/kg intraperitoneally (i.p.) every other day; 4 administrations completed one regimen. Control

mice received a10 ml/kg i.p. injection of the diluent, with the same injection regimen. Seven days after drug treatment, mice were euthanized by decapitation. Lumbar (L4-L6) DRG tissue was collected, immediately frozen in liquid nitrogen, and stored at -80°C until analysis.

Protein isolation

DRG cytoplasmic and membrane enriched protein fractions were obtained as described in [18]. Briefly, DRG specimens were combined with 500 μL of lysis buffer A (NaCl, HEPES, digitonin, hexylene glycol, protease, and phosphatase inhibitor cocktail) and disrupted for 5 seconds using a dounce homogenizer. The resulting tissue suspension was processed with a QIAshredder homogenizer (Qiagen, 79656) and centrifuged at 500g for 10 minutes to filter the homogenate. The pellet was resuspended in 500 μL of lysis buffer A, incubated on a nutator for 10 minutes and centrifuged at 4000g for 10 minutes to isolate the cytosolic proteins. The pellet was resuspended in 1 mL of lysis buffer B (NaCl, HEPES, Igepal, hexylene glycol, protease, and phosphatase inhibitor cocktail), incubated for 30-minutes on a nutator, then centrifuged at 6000g for 10 minutes to collect membrane bound proteins. All centrifugation and incubation steps were performed at 4°C.

Liquid-chromatography electrospray ionization mass spectrometry

Liquid-chromatography electrospray ionization mass spectrometry (LC-ESI MS/MS) was conducted in data-dependent acquisition (DDA) mode similar to previous studies [19, 20]. Briefly, proteins were precipitated by incubating for 5-minutes in acetone on ice followed by centrifugation. Proteins were denatured, reduced, and alkylated in 8 M urea, 1 M dithiothreitol, and 0.5 M iodoacetamide. Proteins were digested in trypsin (0.5 μg/μl) in 500 mM ammonium bicarbonate at 37°C for 5 hours and the fragments were desalted with C-18 ZipTips (Millipore), dehydrated in a SpeedVac for 18 mins, and reconstituted in 0.1% formic acid.

An Exploris Orbitrap 480 equipped with an EASY-nLC 1200 HPLC system (Thermo Fisher Scientific, Waltham, MA, USA) was used to conduct LC-ESI MS/MS analysis. Peptide separation was accomplished using a reverse-phase PepMap RSLC 75 μm i.d by 15 cm long with a 2 μm particle size C18 LC column (Thermo Fisher Scientific, Waltham, MA, USA). A solution of 80% acetonitrile and 0.1% formic acid was used for the peptide elution step at a flow rate of 300 nl/min. A full scan at 60,000 resolving power from 300 m/z to 1200 m/z was followed by peptide fragmentation with high-energy collision dissociation (HCD) at a normalized collision energy of 28%. EASY-IC filters were enabled for internal mass calibration, monoisotopic precursor selection, and dynamic exclusions (20 s). Data were recorded for peptide precursor ions with charge states ranging from +2 to +4. All samples were run in 3 technical replicates.

Proteomic and statistical analysis

Proteins were identified using the SEQUEST HT search engine within Proteome Discoverer v2.4 (Thermo Fisher Scientific, Waltham, MA, USA). Raw MS peptide spectra were compared to the NCBI mouse protein database using specific search engine parameters: mass tolerance for precursor ions of 2 ppm; mass tolerance for fragment ions of 0.05 Da; and a false discovery rate (FDR) cut-off value of 1% for reporting peptide spectrum matches (PSM) to the database. Peptide abundance ratios were calculated by precursor ion quantification in Proteome Discoverer v2.4, using the vehicle control group as the denominator. Statistically significant abundance ratios with adjusted p-values < 0.05 were determined using a Student's t-test. Analysis was performed on proteins with a quantifiable spectra signal profile observed in at least 2 of the 3 technical replicates.

Bioinformatics

Gene ontology (GO) analysis was conducted in the Database for Annotation, Visualization, and Integrated Discovery (DAVID) [21, 22]. The clustering of protein data was conducted using the Search Tool for the Retrieval of Interacting Genes/Proteins (STRING, v11.5) database using a Markov Cluster Algorithm (MCL) with an inflation parameter of 2 [23]. Data was processed, analyzed, and presented using Excel and the following tools: the R statistical software [24] and packages: ggplot2 [25], tidyverse [26].

Results

DRG proteomics characterization in a mouse model of paclitaxel-induced neuropathy

Paclitaxel and other chemotherapy drugs elicit peripheral nerve fiber dysfunction and neurodegeneration that drives PIPN [7]. A few rodent models exist for the study of PIPN including ours [27–29]. In recent studies, we have shown that paclitaxel administration drives altered behaviors including affective states and nociceptive responses such as mechanical allodynia and thermal hyperalgesia within mice [17, 30–34]. To understand the mechanism that may underlie these sensory responses, we assessed proteomic changes from the DRG in response to paclitaxel treatment. Eight adult male mice were treated with either 8 mg/kg body weight paclitaxel every other day for 4 days or 10 ml/kg of the vehicle diluent at the same injection regimen. Whole DRG were obtained from lumbar region L4-L6, an important site for sensory and pain processing [17]. Protein enrichment for cytosolic and membrane proteins was conducted prior to MS analysis. The overall workflow detailing the study is illustrated in **Fig 1**.

Proteomic analysis of DRG was conducted in order to compare changes in protein expression using label free peptide abundance analysis, as previously shown [19, 20]. In these experiments fractions enriched for cytosolic and membrane proteins obtained from the DRG of vehicle treated mice were used as the control. Using LC-ESI MS/MS, we identified a total of 2055 proteins within the cytosolic fraction, and 2676 within the membrane fraction. These proteins are listed in **S1 File**. Statistical analysis of the abundance ratios indicates an effect of paclitaxel on 102 proteins within the membrane fraction and 63 proteins within the cytosolic
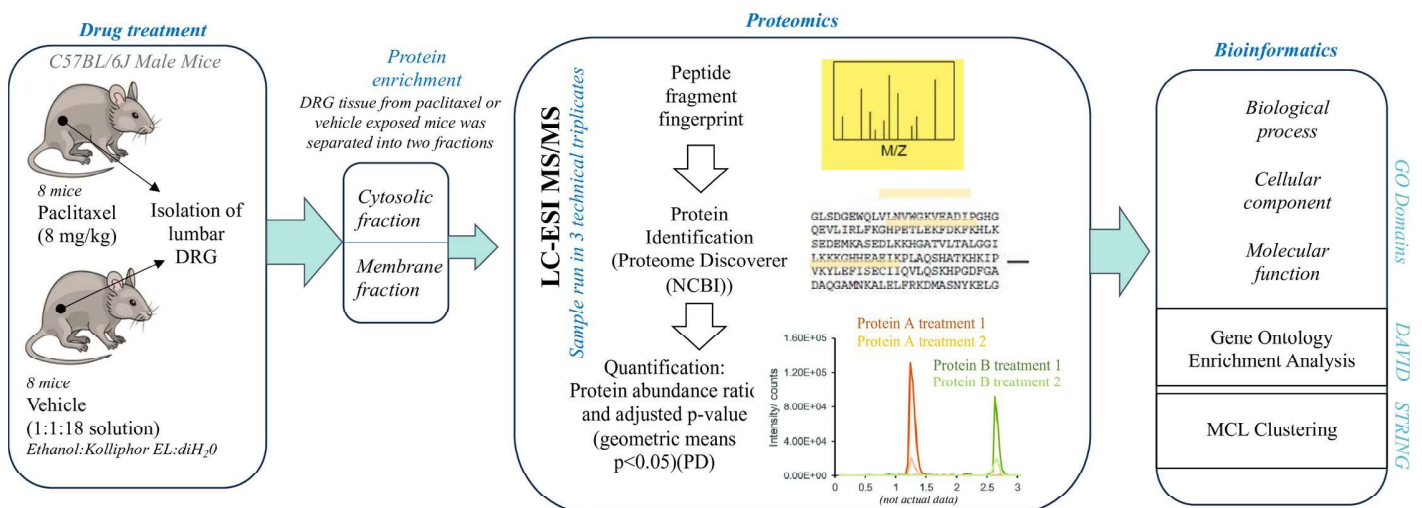

Fig 1. A workflow schematic showing the study design.

https://doi.org/10.1371/journal.pone.0306498.g001

fraction. The list of significantly altered proteins from each cytoplasmic and membrane fraction is presented in **S1 File**. Of the significantly altered proteins, 36 proteins are upregulated while 27 proteins are downregulated in the cytosolic fraction (**Fig 2A**). In addition, 28 proteins were upregulated while 74 are downregulated in the membrane fraction (**Fig 2B**)

We compared our proteomic dataset to published proteomic studies from mouse DRG [35–37]. 88% of proteins identified within our DRG analysis also appear in the DRG proteome of adult mice within pain related studies [37]. Overlapping DRG proteins are shown in **S1 File** [38]. A GO analysis of the significantly altered proteins indicates enrichment of cellular components, molecular functions and biological processes across cytosolic and membrane fraction proteins in the DRG of paclitaxel-treated mice (**Fig 2**). Specifically, cytosolic fraction results indicate an effect of paclitaxel on carbohydrate metabolic processes, lipid metabolism, ATPase function, cytoskeletal intermediate filament and cell adhesion, and cell proliferation as well as apoptosis (**Fig 2C–2E**). Membrane fraction results show an effect of paclitaxel on ATP activity, cell adhesion, cytoskeletal organization, protein transport, and calcium and lipid signaling (**Fig 2F–2H**). GO results appeared to slightly differ however between the two-protein fraction results with cytosolic proteomes highlighting an increase in carbohydrate metabolic processes, while the membrane fraction underscores an effect of paclitaxel on lipid metabolism. GO informatic analysis of the DRG proteome shows an effect of paclitaxel on several important metabolic pathways as well as signaling and structural functions within the DRG.

An effect of paclitaxel on DRG energy, cytoskeletal regulation, and sensory axon signaling

We used DAVID [22, 39] enrichment analysis of GO terms that are associated with significantly altered proteins in both cytosolic and membrane fractions to compare the effect of paclitaxel on DRG proteome adaptation. As shown in **Tables 1 and 2**, enrichment analysis confirms representation of membrane and cytosolic terms within the membrane and cytosolic fractions, respectively. Additionally, enrichment analysis of the membrane fraction indicates a high representation of membrane proteins from various intracellular organelles including the mitochondria as well as the endoplasmic reticulum (ER). Membrane associated proteins are also involved in lipid, metabolic and calcium cell signaling (**Table 2**). We assessed for overlap in significantly altered proteins across the membrane and cytosolic fractions. A subset of significantly altered proteins appeared in both membrane and cytosolic fractions results (**Fig 2I**). These proteins include cluster of differentiation 9 (CD9), myelin basic protein (MBP), calcium binding proteins S100B, parvalbumin (Pvalb),calmodulin, and the cell adhesion molecule SDK1. An analysis of the effect of paclitaxel reveals that some of these overlapping proteins are differentially regulated by the drug treatment condition (**Fig 2I**). These findings suggest an effect of paclitaxel on specific functional proteins within the DRG.

Proteomic analysis can also offer insight into drug-treatment associated adaptations within protein-protein interaction (PPI) networks within target tissue and cell types [40].We used a Markov cluster (MCL) analysis to define PPI networks within the DRG proteome consisting of all significantly upregulated and downregulated proteins from membrane and cytosolic fractions. MCL analysis is represented by an integrated PPI network based on the identity of the significantly altered proteins in response to paclitaxel treatment (**Fig 3**). Within the PPI network we identified 11 high confidence protein clusters. The largest PPI cluster (Cluster 1) was found to contain 14 proteins with 47 connections yielding a significant PPI connection ($p < 1.0 \times 10^{-16}$). It consists of mitochondrial proteins and is positioned centrally within the integrated PPI map (**Fig 3**). Cluster 1 had an average local clustering coefficient (ALCC) of 0.755 with analysis revealing downregulation in this mitochondrial protein network (**Fig 4**).
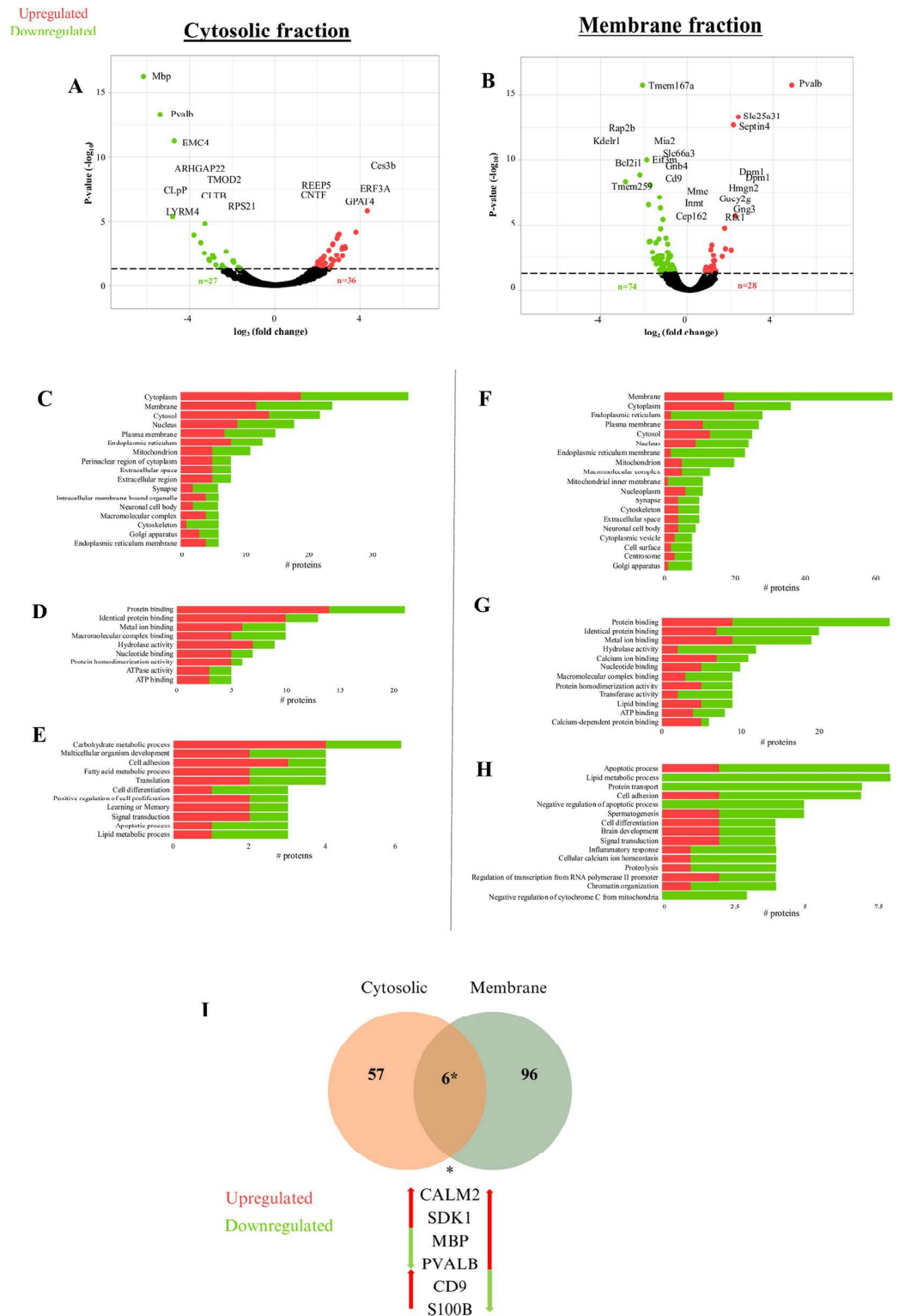
Fig 2. Effect of paclitaxel on the DRG proteome. Volcano plot distribution of significantly altered proteins within the DRG. A) Cytosolic fraction. B) Membrane fraction. GO terms associated with significantly altered proteins in paclitaxel treated mice relative to controls. Cytosolic protein fraction cellular component (C), molecular function (D), biological process. (E). Membrane protein fraction cellular component (F), molecular function (G), biological process (H).

Table 1. DAVID enrichment terms and their associated proteins within the cytosolic fraction.

GO category	Term	Count	Proteins	Adjusted p-value
Cellular component	Cytoplasm	36	YWHAE, MTPN, CNTF, TAGLN, GSPT1, CST3, ARHG AP22, HEBP2, MBP, PTGDS, GET3, EIF4E, PHM1, APC2, TMP3, TMOD2, CDC42BPB, TBCA, S100B, TSN, KIF27, PPP1CA, CARHSP1, RPS28, PSMA4, STK24, NACA, SLMAP, GPD1, G6PDX, GNB3, NAA15, GPD1L, CALM2, RPS21, PVALB	0.009819583
Molecular function	Macromolecular complex binding	10	YWHAE, CNTF, TTR, VAPA, CDC42BPB, ATP5F1D, TSN, ATP5F1E, PVALB, PPP1CA	0.027691179

https://doi.org/10.1371/journal.pone.0306498.t001

The second cluster (Cluster 2) consists of 12 ribosomal proteins that also appear predominantly downregulated within the DRG in response to paclitaxel (**Fig 4**). Additional clusters identified within PPI analysis include cell structural and motility regulators that include cytoskeletal elements (e.g., Clusters 8, 10, 11) and protein clusters involved in biochemical pathways including nitrogen and pyridine metabolism (Clusters 6 and 7).

Discussion

We used a proteomic research strategy to examine molecular changes within the DRG in an established mouse model of PIPN[17, 41]. In recent studies, OMIC methods such as metabolomics, proteomics, and phospho-proteomic analyses were used to identify molecular changes in the DRG during diabetic neuropathy in humans [42]. Our study expands this methodology and assesses the specific impact of paclitaxel on the DRG proteome within a PIPN mouse

Table 2. DAVID enrichment terms and their associated proteins within the membrane fraction.

GO category	Term	Count	Proteins	Adjusted p-value
Cellular component	Membrane	64	LGALS3BP, CLIC4, GOLT1B, KDELR1, ICAM2, MIA2, ATP2A1, FNBP1L, COX7C, TMEM186, CLGN, NDST3, ANXA6, SLC36A1, ENTPD1, MME, SIGMAR1, TAP1, DYNLL1, TLCD3B, MFSD10, DPM1, TMEM256, RAP2B, STIM1, DAD1, GORASP2, TMEM259, NDUFS4, S100A6, CD47, S100A9, CERS2, CDS1, RTN3, STOML2, SLC66A3, MGST3, PON2, DERL1, SLC1A4, ASAP2, HIGD1A, GUCY2G, ZMPSTE24, MTDH, PTDSS2, GNG3, MBP, CD99, MPDUL1, S100A10, NDUFA3, SURF4, ERLINI, SDK1, TSPAN18, CD9, MAN2B1, ESYT2, SLC25A31, CALM2, TOMM5, BCL2L1, CDS2	0.00004
Cellular component	Endoplasmic reticulum	28	CDS1, RTN3, GOLT1B, KDELR1, MGST3, DERL1, MIA2, ATPSA1, CLGN, MTDH, ZMPSTE24, PTDSS2, SLC36A1, RPS7, SURF4, SIGMAR1, ERLIN1, TAP1, TLCD3B, DPM1, STIM1, DAD1, GORASP2, TMEM259, ESYT2, BCL2L1, CERS2, CDS2	0.00000035
Cellular component	Endoplasmic reticulum membrane	23	CDS1, RTN3, KDELR1, SURF4, SIGMAR1, ERLIN1, DERL1, TAP1, MIA2, ATP2A1, TLCD3B, CLGN, MTDH, ZMPSTE24, DPM1, PTDSS2, STIM1, DAD1, GORASP2, TMEM259, ESYT2, CERS2, CDS2	.000000294
Cellular component	Mitochondrion	20	STOML2, CLIC4, NDUFA3, MGST3, TAP1, ATP2A1, SEPTIN4, DYNLL1, HIGD1A, COX7C, TMEM186, TXN2, NDUFS4, ANXA6, ACOT2, PPIF, PMPCB, SLC25A31, TOMM5, BCL2L1	0.030463258
Cellular component	Macromolecular complex	13	PRPS1, RPS7, GOLT1B, ERLINI, HIGD1A, ZMPSTE24, STIM1, ANXA6, GNB4, CD9, MBP, CALM2, PVALB	0.045210595
Cellular component	Mitochondrial inner membrane	11	STOML2, TMEM256, NDUFA3, NDUFS4, PPIF, PMPCB, SLC25A31, HIGD1A, COX7C, TMEM186, BCL2L1	0.0093664559
Molecular function	Lipid binding	9	STOML2, FABP4, APOH, ERLINI, ANXA6, PMP2, ESYT2, MBP, FNBP1L	0.031904593
Molecular function	Calcium-dependent protein binding	6	ANXA6, S100A6, S100B, CALM2, S100A9, S100A10	0.016979225

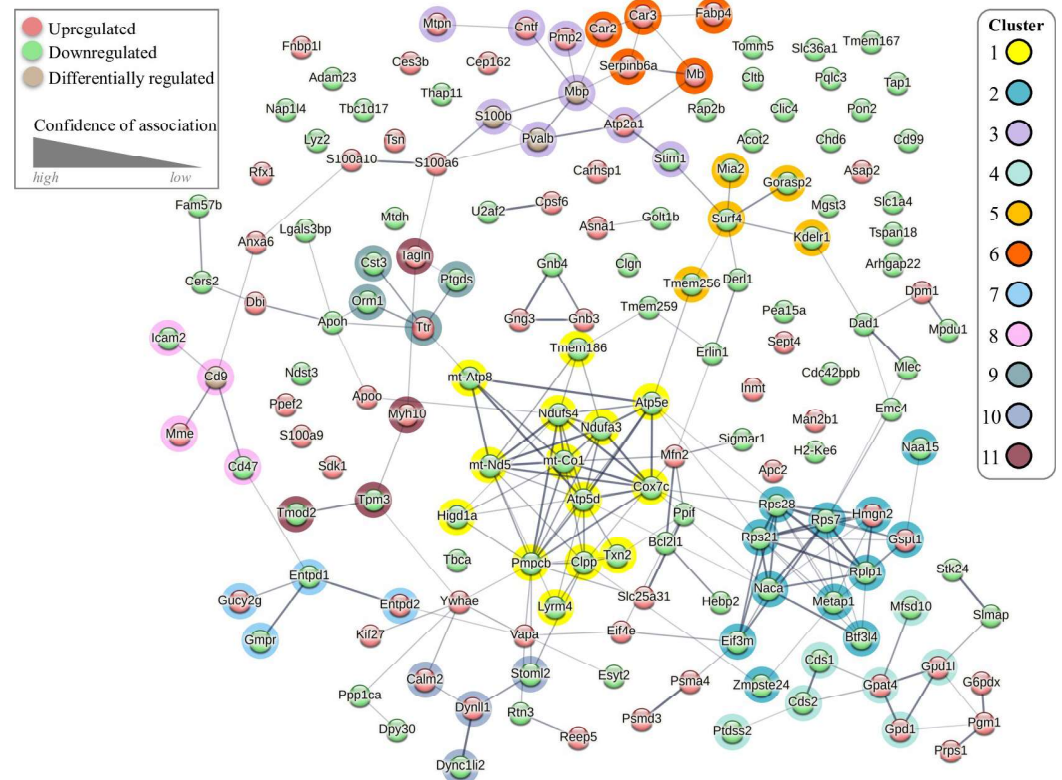https://doi.org/10.1371/journal.pone.0306498.t002

Fig 3. A protein-protein interaction (PPI) map of the paclitaxel associated DRG proteome. STRING network showing PPI amongst all significantly altered proteins. Protein clusters within the network are highlighted by color. The thickness of the connection indicates the degree of confidence between node associations while color indicates whether the protein is increased (red), decreased (green) or differentially altered (light brown) by paclitaxel. The STRING network is based on an MCL algorithm with an inflation parameter of 2 used to identify 11 cluster groups.

https://doi.org/10.1371/journal.pone.0306498.g003

model. Overall, our proteomic results highlight putative disruption to mitochondrial components and related metabolic processes within the DRG during paclitaxel administration, similar to studies that indicate that paclitaxel causes mitochondrial damage in during axonal damage [43–45]. In addition, our findings support the role of paclitaxel in the remodeling of intracellular compartments such as the ER, Golgi, and the cytoskeleton through changes in actin filament and dynein microtubule proteins [44–46]. These results provide evidence on the role of paclitaxel in nervous tissue, and shed light on the potential impact of chemotherapy on DRG associated sensory and neuroimmune activity [47, 48].

Paclitaxel binds to microtubules in both cancer and non-cancer cells impairing cell division as well as other functions. Studies in rodent models show that paclitaxel treatment can also lead to the demyelination and degeneration of axons in nervous tissue [49]. Paclitaxel treatment is also shown to disrupt microtubule transport along axons thereby impairing protein and organelle trafficking within neurons [50, 51]. In particular, paclitaxel's actions appear to correlate with deficits in mitochondrial trafficking in axons both *in vitro* as well as *in vivo* [50, 51] A schematic model of our proteomic findings on DRG function is presented in **Fig 5**. In this model, sensory deficits are suggested to arise as a function of protein changes within multiple cell types and processes in the DRG. In addition, paclitaxel associated proteomic changes may impact sensory signaling outside of the DRG through interactions of sensory axons with target tissue (e.g. epidermis) thereby contributing to pain sensitivity.

Fig 4. Primary cluster groups within the PPI network. An enrichment tag analysis showing the 11 cluster groups within the STRING analysis of the paclitaxel associated DRG proteome.

https://doi.org/10.1371/journal.pone.0306498.g004

Fig 5. A signaling pathway hypothesis model showing the effect of paclitaxel on proteins within the DRG.

https://doi.org/10.1371/journal.pone.0306498.g005

Our model is consistent with evidence on the involvement of DRG connectivity in chemo-therapy associated neuropathy [52]. The DRG contains various sensory neurons, which serve in the processing of sensory information between periphery and CNS. These sensory neurons are encapsulated by a satellite glial cell (SGC) network that modulates neuronal responses to nociception [53]. In addition, immune cells can enter the DRG under heightened inflamma-tory conditions [54]. Our findings support the involvement of neurons and glia in the effect of paclitaxel within the DRG [17] as evidenced by changes in the expression of multiple cell type proteins. For example, Pvalb a calcium binding protein that identifies a subpopulation of pro-prioceptive DRG neurons and has been shown to be associated with peripheral nerve injury [55], is found to be significantly decreased by paclitaxel. S100b on the other hand, a calcium binding protein expressed in glial cells of the DRG [56], is also found to be decreased within the paclitaxel treatment group. These findings point to an effect of paclitaxel on various cell types within the DRG and enables hypothesis to support future mechanistic studies of PIPN.

Bioinformatic analysis of paclitaxel associated proteomic changes within the DRG defines 11 functional network clusters with components that are already known to contribute to pain responses in animal models [57–59]. Our results show proteins across clusters that contribute to enhanced inflammatory responses. For example, changes in the expression of immune cell markers including orosomucoid 1 protein (Orm1), an acute phase inflammatory response pro-tein, and CD47 support evidence on increased neuroimmune activity within the DRG during paclitaxel treatment [60]. Changes in immune cell activity may also contribute to a loss in oli-godendrocyte function including myelin production during neuropathic pain [61]. In support of this, our results show that myelin basic protein (Mbp) is significantly altered within the DRG in response to paclitaxel.

Non-neuronal cells and particularly SGCs are increasingly recognized for their role in the etiology of neuropathic pain. SGC are coupled via gap junctions that are modified by nerve injury as well as neuroinflammation [54]. Chemotherapeutic drugs, such as oxaliplatin or pac-litaxel, have been shown to alter the number of gap junctions between SGCs leading to increased electrical coupling and calcium oscillatory activity within the DRG [62, 63]. In addi-tion, SGC transmit signals bidirectionally between neuron and glia through purinergic (ATP) signaling [64]. Our data shows that Cluster 7 is enriched in purine metabolism proteins that are important for ATP signaling. Changes in ATP sensitivity within the DRG have been previ-ously demonstrated in a mouse pain model with mechanical hypersensitivity and DRG sensory neuron hyperexcitability [45, 65, 66]. An analysis of differentially expressed proteins points to an enrichment of ATP regulators that are associated with mitochondrial activity. The largest of our clusters (Cluster 1) represents mitochondrial proteins including cytochrome C oxidase subunit 7c (Cox7c), mitochondrial encoded cytochrome C oxidase 1 (mt-Co1), thioredoxin 2 (Txn2), and hypoxia-inducible domain family member 1a (Higd1a). Mitochondrial dysfunc-tion is a common feature of neuropathic pain including PIPN [42]. Changes in mitochondrial proteins can impact multiple cell types within the DRG and may influence processes such as schwann cell myelination [67].

Our findings involve nitrogen metabolism (Cluster 6), which fits in with existing research on nitrogen-related compounds in neuropathic pain. Namely, myoglobin (Mb) has been shown to be involved in pain processes [68]. Within this pathway, nitric oxide (NO) is impor-tant in a number of signaling pathways, including immune regulation, neuronal survival, and synaptic plasticity [69], and an overproduction of NO is associated with neuropathic pain [70]. Molecules associated with nitrogen metabolism have been shown to modulate sensory neuron excitability and nociceptive effects [71]. Within Cluster 6, we find that the fatty acid binding protein 4 (FABP4) is significantly increased within the DRG in response to paclitaxel. FABP4 is expressed in adipocytes as well as immune cells such as macrophages and participates in

lipid signaling as well as nitrogen metabolism. Studies show that FABP4 can contribute to neuroinflammation [72].

Our findings provide insight on mechanisms that can contribute to pain responses following paclitaxel treatment within our PIPN model. Our proteomic results are consistent with earlier findings using this mouse model showing an effect of paclitaxel on mechanical and thermal sensitivity. This result is also similar to proteomic studies of paclitaxel associated neuropathy within the rat DRG [41]. Understanding the mechanisms that contribute to PIPN is an important research direction that can be leveraged through combining several OMIC technologies including RNA sequencing (RNAseq) and proteomics withing these important preclinical models.

Supporting information

S1 File.
(DOCX)

Author Contributions

Conceptualization: M. Imad Damaj, Nadine Kabbani.

Data curation: Rania Hanna, Alexandru Graur, Patricia Sinclair.

Formal analysis: Rania Hanna, Alexandru Graur, Patricia Sinclair, Nadine Kabbani.

Funding acquisition: M. Imad Damaj, Nadine Kabbani.

Methodology: Rania Hanna, Alexandru Graur, Bryan D. Mckiver, Paula D. Bos, Nadine Kabbani.

Project administration: M. Imad Damaj, Nadine Kabbani.

Supervision: Nadine Kabbani.

Writing – original draft: Rania Hanna.

Writing – review & editing: Alexandru Graur, Patricia Sinclair, Paula D. Bos, M. Imad Damaj, Nadine Kabbani.

References

1. Belani CP. Paclitaxel and docetaxel combinations in non-small cell lung cancer. Chest. 2000; 117: 144S–151S. https://doi.org/10.1378/chest.117.4_suppl_1.144s PMID: 10777470

2. Nathan FE, Berd D, Sato T, Mastrangelo MJ. Paclitaxel and tamoxifen: An active regimen for patients with metastatic melanoma. Cancer. 2000; 88: 79–87. https://doi.org/10.1002/(sici)1097-0142 (20000101)88:1<79::aid-cncr12>3.0.co;2-l PMID: 10618609

3. Polomano RC, Farrar JT. Pain and neuropathy in cancer survivors. Surgery, radiation, and chemotherapy can cause pain; research could improve its detection and treatment. Am J Nurs. 2006; 106: 39–47. https://doi.org/10.1097/00000446-200603003-00015 PMID: 16481851

4. Kawashiri T, Inoue M, Mori K, Kobayashi D, Mine K, Ushio S, et al. Preclinical and Clinical Evidence of Therapeutic Agents for Paclitaxel-Induced Peripheral Neuropathy. Int J Mol Sci. 2021; 22: 8733. https://doi.org/10.3390/ijms22168733 PMID: 34445439

5. Risinger AL, Riffle SM, Lopus M, Jordan MA, Wilson L, Mooberry SL. The taccalonolides and paclitaxel cause distinct effects on microtubule dynamics and aster formation. Mol Cancer. 2014; 13: 41. https://doi.org/10.1186/1476-4598-13-41 PMID: 24576146

6. Li H-B, Wang W-H, Wang Z-Y. A meta-analysis of the incidence and risk of skin toxicity with nab-paclitaxel and paclitaxel in cancer treatment. Am J Transl Res. 2023; 15: 4279–4290. PMID: 37434856

7. Klein I, Lehmann HC. Pathomechanisms of Paclitaxel-Induced Peripheral Neuropathy. Toxics. 2021; 9: 229. https://doi.org/10.3390/toxics9100229 PMID: 34678925

8. Bhalla KN. Microtubule-targeted anticancer agents and apoptosis. Oncogene. 2003; 22: 9075–9086. https://doi.org/10.1038/sj.onc.1207233 PMID: 14663486

9. Ahimsadasan N, Reddy V, Khan Suheb MZ, Kumar A. Neuroanatomy, Dorsal Root Ganglion. Stat-Pearls. Treasure Island (FL): StatPearls Publishing; 2024. Available: http://www.ncbi.nlm.nih.gov/books/NBK532291/

10. Cervero F, Laird JMA. Mechanisms of touch-evoked pain (allodynia): a new model. Pain. 1996; 68: 13–23. https://doi.org/10.1016/S0304-3959(96)03165-X PMID: 9251994

11. Gornstein EL, Schwarz TL. Neurotoxic mechanisms of paclitaxel are local to the distal axon and independent of transport defects. Exp Neurol. 2017; 288: 153–166. https://doi.org/10.1016/j.expneurol.2016.11.015 PMID: 27894788

12. Fukuda Y, Li Y, Segal RA. A Mechanistic Understanding of Axon Degeneration in Chemotherapy-Induced Peripheral Neuropathy. Front Neurosci. 2017; 11: 481. https://doi.org/10.3389/fnins.2017.00481 PMID: 28912674

13. Vermeer CJC, Hiensch AE, Cleenewerk L, May AM, Eijkelkamp N. Neuro-immune interactions in paclitaxel-induced peripheral neuropathy. Acta Oncol. 2021; 60: 1369–1382. https://doi.org/10.1080/0284186X.2021.1954241 PMID: 34313190

14. Sun W, Yang S, Wu S, Ba X, Xiong D, Xiao L, et al. Transcriptome analysis reveals dysregulation of inflammatory and neuronal function in dorsal root ganglion of paclitaxel-induced peripheral neuropathy rats. Mol Pain. 2022; 19: 17448069221106167. https://doi.org/10.1177/17448069221106167 PMID: 35610945

15. Kim HK, Lee S-Y, Koike N, Kim E, Wirianto M, Burish MJ, et al. Circadian regulation of chemotherapy-induced peripheral neuropathic pain and the underlying transcriptomic landscape. Sci Rep. 2020; 10: 13844. https://doi.org/10.1038/s41598-020-70757-w PMID: 32796949

16. Housley SN, Nardelli P, Carrasco DI, Rotterman TM, Pfahl E, Matyunina LV, et al. Cancer Exacerbates Chemotherapy-Induced Sensory Neuropathy. Cancer Res. 2020; 80: 2940–2955. https://doi.org/10.1158/0008-5472.CAN-19-2331 PMID: 32345673

17. CAILLAUD M, PATEL NH, WHITE A, M WOOD, Contreras KM, TOMA W, et al. Targeting Peroxisome Proliferator-Activated Receptor-α (PPAR- α) to Reduce Paclitaxel-Induced Peripheral Neuropathy. Brain Behav Immun. 2021; 93: 172–185. https://doi.org/10.1016/j.bbi.2021.01.004 PMID: 33434562

18. Baghirova S, Hughes BG, Hendzel MJ, Schulz R. Sequential fractionation and isolation of subcellular proteins from tissue or cultured cells. MethodsX. 2015; 2: 440–445. https://doi.org/10.1016/j.mex.2015.11.001 PMID: 26740924

19. Graur A, Sinclair P, Schneeweis AK, Pak DT, Kabbani N. The human acetylcholinesterase C-terminal T30 peptide activates neuronal growth through alpha 7 nicotinic acetylcholine receptors and the mTOR pathway. Sci Rep. 2023; 13: 11434. https://doi.org/10.1038/s41598-023-38637-1 PMID: 37454238

20. Sinclair P, Kabbani N. Nicotinic receptor components of amyloid beta 42 proteome regulation in human neural cells. Araki W, editor. PLoS ONE. 2022; 17: e0270479. https://doi.org/10.1371/journal.pone.0270479 PMID: 35960729

21. Sherman BT, Hao M, Qiu J, Jiao X, Baseler MW, Lane HC, et al. DAVID: a web server for functional enrichment analysis and functional annotation of gene lists (2021 update). Nucleic Acids Res. 2022; 50: W216–W221. https://doi.org/10.1093/nar/gkac194 PMID: 35325185

22. Huang DW, Sherman BT, Lempicki RA. Systematic and integrative analysis of large gene lists using DAVID bioinformatics resources. Nat Protoc. 2009; 4: 44–57. https://doi.org/10.1038/nprot.2008.211 PMID: 19131956

23. Szklarczyk D, Kirsch R, Koutrouli M, Nastou K, Mehryary F, Hachilif R, et al. The STRING database in 2023: protein–protein association networks and functional enrichment analyses for any sequenced genome of interest. Nucleic Acids Research. 2023; 51: D638–D646. https://doi.org/10.1093/nar/gkac1000 PMID: 36370105

24. R Core Team. R: A language and environment for statistical computing. Vienna, Austria: R Foundation for Statistical Computing; 2021. Available: https://www.R-project.org/

25. Wickham H. ggplot2: Elegant graphics for data analysis. Springer-Verlag, New York; 2016. Available: https://ggplot2.tidyverse.org

26. Wickham H, Averick M, Bryan J, Chang W, McGowan L, François R, et al. Welcome to the Tidyverse. JOSS. 2019; 4: 1686. https://doi.org/10.21105/joss.01686

27. Höke A, Ray M. Rodent Models of Chemotherapy-Induced Peripheral Neuropathy. ILAR Journal. 2014; 54: 273–281. https://doi.org/10.1093/ilar/ilt053 PMID: 24615440

28. Toma W, Caillaud M, Patel NH, Tran TH, Donvito G, Roberts J, et al. N-acylethanolamine-hydrolysing acid amidase: A new potential target to treat paclitaxel-induced neuropathy. European Journal of Pain. 2021; 25: 1367–1380. https://doi.org/10.1002/ejp.1758 PMID: 33675555

29. Toma W, Kyte SL, Bagdas D, Alkhlaif Y, Alsharari SD, Lichtman AH, et al. Effects of paclitaxel on the development of neuropathy and affective behaviors in the mouse. Neuropharmacology. 2017; 117: 305–315. https://doi.org/10.1016/j.neuropharm.2017.02.020 PMID: 28237807

30. Curry ZA, Wilkerson JL, Bagdas D, Kyte SL, Patel N, Donvito G, et al. Monoacylglycerol Lipase Inhibitors Reverse Paclitaxel-Induced Nociceptive Behavior and Proinflammatory Markers in a Mouse Model of Chemotherapy-Induced Neuropathy. J Pharmacol Exp Ther. 2018; 366: 169–183. https://doi.org/10.1124/jpet.117.245704 PMID: 29540562

31. Contreras KM, Caillaud M, Neddenriep B, Bagdas D, Roberts JL, Ulker E, et al. Deficit in voluntary wheel running in chronic inflammatory and neuropathic pain models in mice: Impact of sex and genotype. Behavioural Brain Research. 2021; 399: 113009. https://doi.org/10.1016/j.bbr.2020.113009 PMID: 33181181

32. Kyte SL, Toma W, Bagdas D, Meade JA, Schurman LD, Lichtman AH, et al. Nicotine Prevents and Reverses Paclitaxel-Induced Mechanical Allodynia in a Mouse Model of CIPN. J Pharmacol Exp Ther. 2018; 364: 110–119. https://doi.org/10.1124/jpet.117.243972 PMID: 29042416

33. Meade JA, Alkhlaif Y, Contreras KM, Obeng S, Toma W, Sim-Selley LJ, et al. Kappa opioid receptors mediate an initial aversive component of paclitaxel-induced neuropathy. Psychopharmacology (Berl). 2020; 237: 2777–2793. https://doi.org/10.1007/s00213-020-05572-2 PMID: 32529265

34. Xu L, Chen X, Wang L, Han J, Wang Q, Liu S, et al. Paclitaxel combined with platinum (PTX) versus fluorouracil combined with cisplatin (PF) in the treatment of unresectable esophageal cancer: a systematic review and meta-analysis of the efficacy and toxicity of two different regimens. J Gastrointest Oncol. 2023; 14: 1037–1051. https://doi.org/10.21037/jgo-23-33 PMID: 37201087

35. Schwaid AG, Krasowka-Zoladek A, Chi A, Cornella-Taracido I. Comparison of the Rat and Human Dorsal Root Ganglion Proteome. Sci Rep. 2018; 8: 13469. https://doi.org/10.1038/s41598-018-31189-9 PMID: 30194433

36. Leal-Julià M, Vilches JJ, Onieva A, Verdés S, Sánchez Á, Chillón M, et al. Proteomic quantitative study of dorsal root ganglia and sciatic nerve in type 2 diabetic mice. Mol Metab. 2021; 55: 101408. https://doi.org/10.1016/j.molmet.2021.101408 PMID: 34856394

37. Pogatzki-Zahn EM, Gomez-Varela D, Erdmann G, Kaschube K, Segelcke D, Schmidt M. A proteome signature for acute incisional pain in dorsal root ganglia of mice. Pain. 2021; 162: 2070–2086. https://doi.org/10.1097/j.pain.0000000000002207 PMID: 33492035

38. Venny 2.1.0. [cited 7 Jun 2024]. Available: https://bioinfogp.cnb.csic.es/tools/venny/

39. Sherman BT, Hao M, Qiu J, Jiao X, Baseler MW, Lane HC, et al. DAVID: a web server for functional enrichment analysis and functional annotation of gene lists (2021 update). Nucleic Acids Research. 2022; 50: W216–W221. https://doi.org/10.1093/nar/gkac194 PMID: 35325185

40. Dengjel J, Kratchmarova I, Blagoev B. Mapping Protein–Protein Interactions by Quantitative Proteomics. In: Cutillas PR, Timms JF, editors. LC-MS/MS in Proteomics. Totowa, NJ: Humana Press; 2010. pp. 267–278. https://doi.org/10.1007/978-1-60761-780-8_16 PMID: 20839110

41. de Clauser L, Kappert C, Sondermann JR, Gomez-Varela D, Flatters SJL, Schmidt M. Proteome and Network Analysis Provides Novel Insights Into Developing and Established Chemotherapy-Induced Peripheral Neuropathy. Front Pharmacol. 2022; 13: 818690. https://doi.org/10.3389/fphar.2022.818690 PMID: 35250568

42. Doty M, Yun S, Wang Y, Hu M, Cassidy M, Hall B, et al. Integrative multiomic analyses of dorsal root ganglia in diabetic neuropathic pain using proteomics, phospho-proteomics, and metabolomics. Sci Rep. 2022; 12: 17012. https://doi.org/10.1038/s41598-022-21394-y PMID: 36220867

43. Cirrincione AM, Pellegrini AD, Dominy JR, Benjamin ME, Utkina-Sosunova I, Lotti F, et al. Paclitaxel-induced peripheral neuropathy is caused by epidermal ROS and mitochondrial damage through conserved MMP-13 activation. Sci Rep. 2020; 10: 3970. https://doi.org/10.1038/s41598-020-60990-8 PMID: 32132628

44. Canta A, Pozzi E, Carozzi VA. Mitochondrial Dysfunction in Chemotherapy-Induced Peripheral Neuropathy (CIPN). Toxics. 2015; 3: 198–223. https://doi.org/10.3390/toxics3020198 PMID: 29056658

45. Duggett NA, Griffiths LA, Flatters SJL. Paclitaxel-induced painful neuropathy is associated with changes in mitochondrial bioenergetics, glycolysis, and an energy deficit in dorsal root ganglia neurons. Pain. 2017; 158: 1499–1508. https://doi.org/10.1097/j.pain.0000000000000939 PMID: 28541258

46. Bennett GJ, Doyle T, Salvemini D. Mitotoxicity in distal symmetrical sensory peripheral neuropathies. Nat Rev Neurol. 2014; 10: 326–336. https://doi.org/10.1038/nrneurol.2014.77 PMID: 24840972

47. Huang Z-Z, Li D, Liu C-C, Cui Y, Zhu H-Q, Zhang W-W, et al. CX3CL1-mediated macrophage activation contributed to paclitaxel-induced DRG neuronal apoptosis and painful peripheral neuropathy. Brain, Behavior, and Immunity. 2014; 40: 155–165. https://doi.org/10.1016/j.bbi.2014.03.014 PMID: 24681252

48. Zhang H, Li Y, De Carvalho-Barbosa M, Kavelaars A, Heijnen CJ, Albrecht PJ, et al. Dorsal Root Ganglion Infiltration by Macrophages Contributes to Paclitaxel Chemotherapy-Induced Peripheral Neuropathy. The Journal of Pain. 2016; 17: 775–786. https://doi.org/10.1016/j.jpain.2016.02.011 PMID: 26979998

49. Woo DDL, Miao SYP, Pelayo JC, Woolf AS. Taxol inhibits progression of congenital polycystic kidney disease. Nature. 1994; 368: 750–753. https://doi.org/10.1038/368750a0 PMID: 7908721

50. Benbow SJ, Wozniak KM, Kulesh B, Savage A, Slusher BS, Littlefield BA, et al. Microtubule Targeting Agents Eribulin and Paclitaxel Differentially Affect Neuronal Cell Bodies in Chemotherapy Induced Peripheral Neuropathy. Neurotox Res. 2017; 32: 151–162. https://doi.org/10.1007/s12640-017-9729-6 PMID: 28391556

51. Flatters SJL, Bennett GJ. Studies of peripheral sensory nerves in paclitaxel-induced painful peripheral neuropathy: Evidence for mitochondrial dysfunction. Pain. 2006; 122: 245–257. https://doi.org/10.1016/j.pain.2006.01.037 PMID: 16530964

52. Talagas M, Lebonvallet N, Leschiera R, Marcorelles P, Misery L. What about physical contacts between epidermal keratinocytes and sensory neurons? Experimental Dermatology. 2018; 27: 9–13. https://doi.org/10.1111/exd.13411 PMID: 28767170

53. Nedergaard M, Ransom B, Goldman SA. New roles for astrocytes: Redefining the functional architecture of the brain. Trends in Neurosciences. 2003; 26: 523–530. https://doi.org/10.1016/j.tins.2003.08.008 PMID: 14522144

54. JASMIN L, VIT J-P, BHARGAVA A, OHARA PT. Can satellite glial cells be therapeutic targets for pain control? Neuron Glia Biol. 2010; 6: 63–71. https://doi.org/10.1017/S1740925X10000098 PMID: 20566001

55. Walters MC, Ladle DR. Calcium homeostasis in parvalbumin DRG neurons is altered after sciatic nerve crush and sciatic nerve transection injuries. J Neurophysiol. 2021; 126: 1948–1958. https://doi.org/10.1152/jn.00707.2020 PMID: 34758279

56. Costa FAL, Moreira Neto FL. [Satellite glial cells in sensory ganglia: its role in pain]. Rev Bras Anestesiol. 2015; 65: 73–81. https://doi.org/10.1016/j.bjan.2013.07.013 PMID: 25497752

57. Facer P, Casula MA, Smith GD, Benham CD, Chessell IP, Bountra C, et al. Differential expression of the capsaicin receptor TRPV1 and related novel receptors TRPV3, TRPV4 and TRPM8 in normal human tissues and changes in traumatic and diabetic neuropathy. BMC Neurol. 2007; 7: 11. https://doi.org/10.1186/1471-2377-7-11 PMID: 17521436

58. Han Q, Kim YH, Wang X, Liu D, Zhang Z-J, Bey AL, et al. SHANK3 Deficiency Impairs Heat Hyperalgesia and TRPV1 Signaling in Primary Sensory Neurons. Neuron. 2016; 92: 1279–1293. https://doi.org/10.1016/j.neuron.2016.11.007 PMID: 27916453

59. Wilder-Smith CH. Abnormal endogenous pain modulation and somatic and visceral hypersensitivity in female patients with irritable bowel syndrome. WJG. 2007; 13: 3699. https://doi.org/10.3748/wjg.v13.i27.3699 PMID: 17659729

60. Yu X, Liu H, Hamel KA, Morvan MG, Yu S, Leff J, et al. Dorsal root ganglion macrophages contribute to both the initiation and persistence of neuropathic pain. Nat Commun. 2020; 11: 264. https://doi.org/10.1038/s41467-019-13839-2 PMID: 31937758

61. Klein I, Boenert J, Lange F, Christensen B, Wassermann MK, Wiesen MHJ, et al. Glia from the central and peripheral nervous system are differentially affected by paclitaxel chemotherapy via modulating their neuroinflammatory and neuroregenerative properties. Front Pharmacol. 2022; 13: 1038285. https://doi.org/10.3389/fphar.2022.1038285 PMID: 36408236

62. Huang T-Y, Belzer V, Hanani M. Gap junctions in dorsal root ganglia: Possible contribution to visceral pain. European Journal of Pain. 2010; 14: 49.e1–49.e9. https://doi.org/10.1016/j.ejpain.2009.02.005 PMID: 19345595

63. Warwick R a., Hanani M. The contribution of satellite glial cells to chemotherapy-induced neuropathic pain. European Journal of Pain. 2013; 17: 571–580. https://doi.org/10.1002/j.1532-2149.2012.00219.x PMID: 23065831

64. Suadicani SO, Cherkas PS, Zuckerman J, Smith DN, Spray DC, Hanani M. Bidirectional calcium signaling between satellite glial cells and neurons in cultured mouse trigeminal ganglia. Neuron Glia Biol. 2010; 6: 43–51. https://doi.org/10.1017/S1740925X09990408 PMID: 19891813

65. Kushnir R, Cherkas PS, Hanani M. Peripheral inflammation upregulates P2X receptor expression in satellite glial cells of mouse trigeminal ganglia: A calcium imaging study. Neuropharmacology. 2011; 61: 739–746. https://doi.org/10.1016/j.neuropharm.2011.05.019 PMID: 21645532

66. Mikesell AR, Isaeva E, Schulte ML, Menzel AD, Sriram A, Prahl MM, et al. Keratinocyte Piezo1 drives paclitaxel-induced mechanical hypersensitivity. bioRxiv. 2023; 2023.12.12.571332. https://doi.org/10.1101/2023.12.12.571332 PMID: 38168305

67. Komori N, Takemori N, Kim HK, Singh A, Hwang S-H, Foreman RD, et al. Proteomics study of neuropathic and nonneuropathic dorsal root ganglia: altered protein regulation following segmental spinal nerve ligation injury. Physiological Genomics. 2007; 29: 215–230. https://doi.org/10.1152/physiolgenomics.00255.2006 PMID: 17213366

68. Gerdle B, Ghafouri B. Proteomic studies of common chronic pain conditions—a systematic review and associated network analyses. Expert Review of Proteomics. 2020; 17: 483–505. https://doi.org/10.1080/14789450.2020.1797499 PMID: 32684010

69. Ahlawat A, Rana A, Goyal N, Sharma S. Potential role of nitric oxide synthase isoforms in pathophysiology of neuropathic pain. Inflammopharmacology. 2014; 22: 269–278. https://doi.org/10.1007/s10787-014-0213-0 PMID: 25095760

70. Hara MR, Snyder SH. Cell Signaling and Neuronal Death. Annual Review of Pharmacology and Toxicology. 2007; 47: 117–141. https://doi.org/10.1146/annurev.pharmtox.47.120505.105311 PMID: 16879082

71. Hamza M, Wang X-M, Wu T, Brahim JS, Rowan JS, Dionne RA. Nitric oxide is negatively correlated to pain during acute inflammation. Mol Pain. 2010; 6: 55. https://doi.org/10.1186/1744-8069-6-55 PMID: 20843331

72. Peng X, Studholme K, Kanjiya MP, Luk J, Bogdan D, Elmes MW, et al. Fatty-acid-binding protein inhibition produces analgesic effects through peripheral and central mechanisms. Mol Pain. 2017; 13: 1744806917697007. https://doi.org/10.1177/1744806917697007 PMID: 28326944